Front. Phys., 2011, 6(1): 100–105
DOI 10.1007/s11467-010-0148-x

RESEARCH ARTICLE

Gluon number fluctuations and diffusive scaling effect

Wolfgang FISCHER†

Department of Physics, Bielefeld University of Applied Sciences, Bielefeld 33615, Germany

E-mail: †*wfischerphy@gmail.com*

Received August 31, 2010; accepted October 30, 2010

The diffusive scaling is studied based on pomeron loop equations in the fixed coupling case. At $Y \gg Y_{\rm DS}$, the gluon number fluctuations become important, the geometric scaling is replaced by the diffusive scaling. In the diffusive scaling regime, the deep inelastic scattering (DIS) total scattering cross-section is a function of single variable $\ln[1/(r^2Q_s^2(x))]/\sqrt{DY}$. We show that the deep inelastic scattering experimental data lie on a single curve, which seems to indicate the existence of the diffusive scaling phenomenology in the deep inelastic scattering.

Keywords gluon number fluctuations, proton structure function, pomeron loop

PACS numbers 12.38.Aw, 13.85.Fb, 13.60.-r

1 Introduction

There has been a tremendous theoretical progress in understanding the high energy QCD evolution beyond the mean field approximation, i.e. beyond the Balitsky–Kovchgov (BK) equation [1–4], in last few years. It has shown that the particle number fluctuations are important in the evolution of the wave function of a hadron from a dilute regime to a high density regime [5–7]. Also, in Ref. [8] Iancu and Mueller found that the fluctuations slow down the evolution of scattering amplitude near the unitarity limit as compared to the scattering amplitude resulting from the BK equation [1–4]. Mueller and Shoshi have established in Ref. [9] a groundbreaking work beyond the mean field approximation by extending the Kovchegov equation by taking into account the discreteness of gluon numbers. They found that the discreteness of gluon numbers brings in a large correction for the rapidity dependence of the saturation momentum and makes the scattering amplitude violate the geometric scaling. Their work has triggered further developments in small x physics. Later on a relation between high energy QCD evolution and reaction diffusion processes in statistical physics has been set up [10], which shows that the results obtained in Ref. [9] are similar to those emerging in the reaction diffusion processes in statistical physics. The outcomes in Ref. [10] clarify even further that the discreteness of gluon numbers and the gluon number fluctuations are very important in the low parton density regime and are the new elements in the course of the evolution [11].

Soon after the first breakthroughs in understanding the high energy QCD evolution beyond the mean field approximation, it was realized in Refs. [12–15] that both the BK and the Jalilian–Marian, Iancu, McLerran, Weget, Leonidov and Kovner (JIMWLK) equations [16–21] do not properly describe the evolution of a wave function of a hadron in the low parton density regime where the fluctuations in gluon numbers become important, as they include only the Pomeron splittings (BK) and Pomeron mergings (JIMWLK) but not Pomeron mergings (BK) and Pomeron splittings (JIMWLK), respectively (depending upon the perspective from which one views the evolution), therefore they miss the Pomeron loops in the course of the evolution. The Kovchegov or JIMWLK equations have been extended by Pomeron loops and new equations have emerged, the so-called Pomeron loop equations [12–14]. One of the main hallmarks of the Pomeron loop equations is the so-called *diffusive scaling* behavior of the scattering amplitude T, namely, T is a function of a single variable $\ln[1/(r^2Q_s^2(Y))]/\sqrt{DY}$ [22], where D is the diffusion coefficient.

In this paper, we will simply review the dipole picture of deep inelastic scattering in Section 2. The total cross-section of a virtual photon scattering off a proton will be computed in the dipole frame. In Section 3, we will recall the geometric scaling property of the total cross-section of the deep inelastic scattering, where the total cross-section is a function of a single variable, $r^2Q_s^2(Y)$, instead of depending on $\boldsymbol{r}$ and Y separately. The gluon number fluctuations and diffusive scaling will be discussed in Section 4. It will show that in the case of gluon number

fluctuation geometric scaling from the BK equation is replaced by a new scaling, the diffusive scaling, namely the total cross-section of the deep inelastic scattering is a function of a single $\ln[1/(r^2Q_s^2(Y))]/\sqrt{DY}$. Finally, we give the possible implication of diffusive scaling at deep inelastic scattering in Section 5. We do see that the data points lie on a single curve, which indicate the possible diffusive scaling in the present available deep inelastic scattering data.

2 Dipole picture of deep inelastic scattering

Deep inelastic scattering is a process wherein a virtual photon is to be used as a hard probe to explore the structure inside a proton and investigate its partonic constitutes, like quarks and gluons which comply with the law of perturbative quantum chromodynamics (QCD), see Fig. 1. To compute the total cross-section of deep inelastic scattering in high-energy limit, it is better to view the deep inelastic scattering process in a particular frame called the projectile frame or target frame. To simplify computation, we will do our work only in the projectile (dipole) frame in this paper. I would like to note that one can get the exact same results in the target frame. In the projectile frame, the virtual photon fluctuates into a colorless $q\bar{q}$ pair, usually called a dipole, which will interact with the target proton. The probability of a virtual photon fluctuation into a $q\bar{q}$ dipole is computable from QED, which is obtained via the $q\bar{q}$ component of the wave-function, $\psi(\boldsymbol{r}, z, Q^2)$, of the virtual photon. The wave-function depends on two-dimensional vector $\boldsymbol{r}$ whose modulus is the transverse size of the $q\bar{q}$ dipole, virtuality Q^2, and the longitudinal momentum fraction z. It is easy to find the formulae of wave-function, $\psi(\boldsymbol{r}, z, Q^2)$, in the literature [23, 24]

$$|\psi_T^{(f)}(\boldsymbol{r}, z, Q^2)|^2 = e_f^2 \frac{\alpha_e N_c}{2\pi^2}\{[z^2 + (1-z)^2]\bar{Q}_f^2 \cdot K_1^2(r\bar{Q}_f^2) + m_f^2 K_0^2(r\bar{Q}_f^2)\} \quad (1)$$

$$|\psi_L^{(f)}(\boldsymbol{r}, z, Q^2)|^2 = e_f^2 \frac{\alpha_e N_c}{2\pi^2} 4Q^2 z^2 (1-z)^2 K_0^2(r\bar{Q}_f^2) \quad (2)$$

where the e_f and m_f denote the charge and mass of the quark with flavor f and $\bar{Q}_f^2 = z(1-z)Q^2 + m_f^2$.

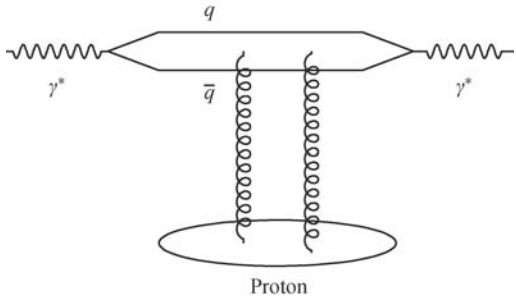

Fig. 1 Deep inelastic scattering.

Now, let us compute the total cross-section of the deep inelastic scattering. In terms of the optical theorem we know that the total cross-section is related to the elastic scattering of the virtual photon. In the dipole frame the deep inelastic scattering proceeds as: the virtual photon splits into a dipole with transverse size $\boldsymbol{r}$, then it scatters elastically with the target proton at a given impact parameter $\boldsymbol{b}$; finally, the dipole recombines back into the virtual photon. The overlap function, ϕ_λ, in the calculation of the total cross-section is

$$\phi_\lambda(\boldsymbol{r}, z, Q^2) = N_c \sum_f [\psi^{(f)}(\boldsymbol{r}, z, Q^2)]^* \psi^{(f)}(\boldsymbol{r}, z, Q^2) \quad (3)$$

where λ denotes the polarization orientation of the virtual photon. In the fixed impact parameter $\boldsymbol{b}$ case, the total cross-section is the given by

$$\frac{\mathrm{d}\sigma_{\mathrm{tot}}}{\mathrm{d}^2 b}(x, Q^2) = 2\int \mathrm{d}^2 r \int_0^1 \mathrm{d}z \sum_{\lambda=T,L} \phi_\lambda(\boldsymbol{r}, z, Q^2) \cdot T_{q\bar{q}}(\boldsymbol{r}, \boldsymbol{b}, x) \quad (4)$$

The interesting ingredient for us in Eq. (4) is the scattering amplitude, $T_{q\bar{q}}(\boldsymbol{r}, \boldsymbol{b}, x)$, of the $q\bar{q}$ dipole of size $\boldsymbol{r}$ off the proton at impact parameter $\boldsymbol{b}$. The x dependence of the $T_{q\bar{q}}(\boldsymbol{r}, \boldsymbol{b}, x)$ reflects the fact that in the dipole frame, the proton carries all the energy and is evolved up to rapidity, $Y = \ln(1/x)$.

3 Geometrical scaling

The evolution equation obtained in the mean field approximation is the Balitsky–Kovchegov (BK) equation [1–4],

$$\frac{\partial}{\partial Y} T(x_\perp - y_\perp, Y) = \frac{\alpha N_c}{2\pi^2} \int \mathrm{d}^2 z_\perp \cdot \frac{(x_\perp - y_\perp)^2}{(x_\perp - z_\perp)^2 (z_\perp - y_\perp)^2} \cdot [T(x_\perp - z_\perp, Y) T(z_\perp - y_\perp, Y) - T(x_\perp - y_\perp, Y)] \quad (5)$$

where $x_\perp - y_\perp$ is the transverse size of initial quark-antiquark dipole, and $x_\perp - z_\perp$ and $z_\perp - y_\perp$ denote the size of two daughter dipoles decayed from the initial $q\bar{q}$ dipole. The BK equation gives the rapidity evolution of the scattering amplitude, $T(x_\perp - y_\perp, Y)$, of a $q\bar{q}$ dipole off a target which can be another dipole, a hadron or a nucleus. The BK equation is a simple equation to deal with the onset of unitarity and to study parton saturation phenomena at high energies. The analytic solution to the fixed coupling BK equation for the T deep in the saturation regime has been derived by Levin and Tuchin [25]. This solution agrees with the one derived by solving the BK equation in the small T limit [26, 27].

One of the hallmarks of the BK equation is the geometrical scaling behavior of the T in large kinematical windows,

$$T(\boldsymbol{r},\boldsymbol{b},x)=S(\boldsymbol{b})T(\boldsymbol{r}^2Q_s^2(x)) \tag{6}$$

with the saturation momentum $Q_s(x)$ defined by $T(r\simeq 1/Q_s,x)$ to be constant of order 1. Equation (6) shows that at small values of x, instead of being a function of a priori two variables $\boldsymbol{r}$ and x, $T(\boldsymbol{r},\boldsymbol{b}\simeq 0,x)$ is actually a function of a single variable $\boldsymbol{r}^2Q_s^2(x)$ up to an inverse dipole size significantly larger than the saturation scale $Q_s(x)$. In Eq. (6), we introduce the impact parameter dependence via a profile function $S(\boldsymbol{b})$. Usually, $S(\boldsymbol{b})=\exp(-\boldsymbol{b}^2/R_p^2)$ with transverse radius of the proton, R_p. Actually, the impact parameter contributes only to the normalization via a constant factor $\int \mathrm{d}^2bS(\boldsymbol{b})=C$.

The geometric scaling behavior in Eq. (6) indicates a similar geometric scaling for the deep inelastic scattering total cross-section

$$\sigma_{\mathrm{tot}}(x,Q^2)=\sigma_{\mathrm{tot}}(\tau) \tag{7}$$

with

$$\tau=Q^2/Q_s^2(x) \tag{8}$$

The geometric scaling has been confirmed by HERA data with $Q_s(x)$ given by

$$Q_s^2(x)=Q_0^2\left(\frac{x}{x_0}\right)^{\lambda} \tag{9}$$

with reference scale $Q_0=1$ GeV, and the parameters $x_0=3.04\times10^{-4}$ and $\lambda=0.288$ [29]. Figure 2 shows that the total cross-section σ_{tot} is a function of τ. The data are taken from different experiments with $x<0.01$, the ZEUS [30, 31], H1 [28], E665 [32] and NMC [33] collaborations. The data lie on the same curve except serval data points taken from the E665 experiment.

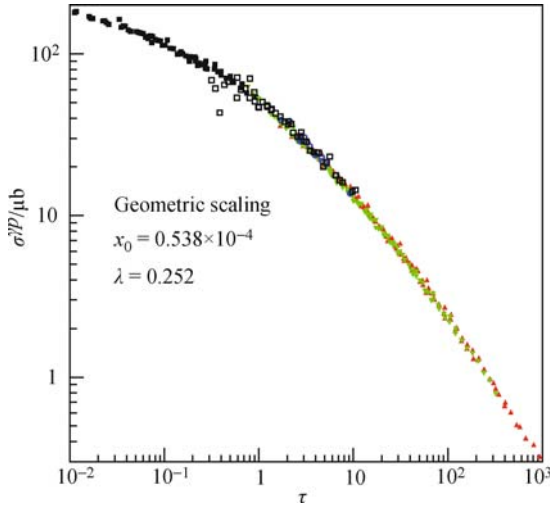

Fig. 2 The total cross-section σ_{tot} is a function of a single variable τ. The experimental data take from ZEUS, H1, E665 and NMC collaborations.

4 Gluon number fluctuations and diffusive scaling

One of shortcomings of the BK equation is that the BK equation does not include fluctuations. However, it took some time to realize that the Balitsky–JIMWLK [1, 2, 16–21] equations also miss them. It turned out that the Balitsky–JIMWLK equations do include linear evolution (Balitsky–Fadin–Kuraev–Lipatov evolution) [34, 35], and pomeron mergings but not pomeron splittings [36]. It was shown that the BK equation and Balitsky-JIMWLK equations are equivalent to each other [37]. Therefore, both of them do not include gluon number fluctuations. After realizing absent fluctuations in the BK equation and Balitsky–JIMWLK equations, the so-called pomeron loop equations have been constructed to account for pomeron splitting or fluctuation in gluon numbers.

4.1 Pomeron loop equations

When one takes into account the Pomeron loop effects in the high energy QCD evolution, the Pomeron loop equations can be written as [14]:

$$\begin{aligned}
\frac{\partial\langle T(x_\perp,y_\perp)\rangle_Y}{\partial Y}&=\frac{\bar\alpha_s}{2\pi}\int \mathrm{d}^2z_\perp\{\mathcal{M}_{x_\perp y_\perp z_\perp}\otimes\langle T(x_\perp,y_\perp)\rangle_Y-\mathcal{M}(x_\perp,y_\perp,z_\perp)\cdot\langle T^{(2)}(x_\perp,z_\perp;z_\perp,y)\rangle_Y\}\\
\frac{\partial\langle T^{(2)}(x_{\perp1},y_{\perp1};x_{\perp2},y_{\perp2})\rangle_Y}{\partial Y}&=\frac{\bar\alpha_s}{2\pi}\int \mathrm{d}^2z_\perp\{[\mathcal{M}_{x_{\perp1},y_{\perp1},z_\perp}\otimes\langle T^{(2)}(x_{\perp1},y_{\perp1};x_{\perp2},y_{\perp2})\rangle_Y-\mathcal{M}(x_{\perp1},y_{\perp1},z_\perp)\\
&\quad\cdot\langle T^{(3)}(x_{\perp1},z_\perp;z_\perp,y_{\perp1};x_{\perp2},y_{\perp2})\rangle_Y\Big]\\
&\quad+[1\leftrightarrow2]\}+\left.\frac{\partial\langle T^{(2)}(x_{\perp1},y_{\perp1};x_{\perp2},y_{\perp2})\rangle_Y}{\partial Y}\right|_{\mathrm{fluct}}\cdots
\end{aligned} \tag{10}$$

with

$$\begin{aligned}
\left.\frac{\partial\langle T^{(2)}(x_{\perp1},y_{\perp1};x_{\perp2},y_{\perp2})\rangle_Y}{\partial Y}\right|_{\mathrm{fluct}}&=\left(\frac{\alpha_s}{2\pi}\right)^2\frac{\bar\alpha_s}{2\pi}\int \mathrm{d}^2u_\perp\mathrm{d}^2v_\perp\mathrm{d}^2z_\perp\mathcal{M}(u_\perp,v_\perp,z_\perp)\\
&\quad\cdot\mathcal{A}_{dd}(x_{\perp1},y_{\perp1}|u_\perp,z_\perp)\mathcal{A}_{dd}(x_{\perp2},y_{\perp2}|z_\perp,v_\perp)\\
&\quad\cdot\nabla^2_{u_\perp}\nabla^2_{v_\perp}\langle T(u_\perp,v_\perp)\rangle_Y
\end{aligned} \tag{11}$$

where the dipole kernel is

$$\mathcal{M}(x_\perp,y_\perp,z_\perp)=\frac{(x_\perp-y_\perp)^2}{(x_\perp-z_\perp)^2(z_\perp-y_\perp)^2} \tag{12}$$

and

$$\mathcal{M}_{x_\perp,y_\perp,z_\perp}\otimes f(x_\perp,y_\perp)\equiv\mathcal{M}(x_\perp,y_\perp,z_\perp)\,[-f(x_\perp,y_\perp)+f(x_\perp,z_\perp)+f(z_\perp,y_\perp)] \tag{13}$$

and $\mathcal{A}_{\rm dd}$ is the amplitude for dipole–dipole scattering and for a large N_c

$$\mathcal{A}_{\rm dd}(x_\perp,y_\perp|u_\perp,v_\perp)=\frac{\alpha_s^2}{8}\left[\ln\frac{(x_\perp-v_\perp)^2(y_\perp-u_\perp)^2}{(x_\perp-u_\perp)^2(y_\perp-v_\perp)^2}\right]^2 \tag{14}$$

Here, $x_\perp, y_\perp, z_\perp, u_\perp$ and $v_\perp$ are the transverse coordinates of the dipoles.

We would like to note that the Pomeron loop equations can equivalently be written as a single stochastic equation of Langevin type [14],

$$\frac{\partial T_Y(x_\perp,y_\perp)}{\partial Y}=\frac{\bar\alpha_s}{2\pi}\int {\rm d}^2z_\perp[\mathcal{M}_{x_\perp,y_\perp,z_\perp}\otimes T_Y(x_\perp,y_\perp) -\mathcal{M}(x_\perp,y_\perp,z_\perp)T_Y(x_\perp,z_\perp) \cdot T_Y(z_\perp,y_\perp)]+\left.\frac{\partial T_Y(x_\perp,y_\perp)}{\partial Y}\right|_{\rm fluct} \tag{15}$$

with the noise term

$$\left.\frac{\partial T_Y(x_\perp,y_\perp)}{\partial Y}\right|_{\rm fluct}=\frac{\alpha_s}{2\pi}\sqrt{\frac{\bar\alpha_s}{2\pi}}\int {\rm d}^2u_\perp{\rm d}^2v_\perp{\rm d}^2z_\perp \cdot\mathcal{A}_{\rm dd}(x_\perp,y_\perp|u_\perp,z_\perp)\frac{|u_\perp-v_\perp|}{(u_\perp-z_\perp)^2} \cdot\sqrt{\nabla^2_{u_\perp}\nabla^2_{v_\perp}T_Y(u_\perp,v_\perp)}\nu(u_\perp,v_\perp,z_\perp,Y) \tag{16}$$

where the noise satisfies

$$\langle\nu(u_{\perp1},v_{\perp1},z_{\perp1},Y)\nu(u_{\perp2},v_{\perp2},z_{\perp2},Y')\rangle =\delta^{(2)}(u_{\perp1}-v_{\perp2})\delta^{(2)}(v_{\perp1}-u_{\perp2}) \cdot\delta^{(2)}(z_{\perp1}-z_{\perp2})\delta(Y-Y') \tag{17}$$

The noise term clarifies that the Pomeron loop equations take into account gluon number fluctuations.

4.1 Correspondences between high density QCD and statistical physics

Consider a dipole with variable size r_0 scattering off another dipole with size r_1. In the dipole frame, the target carries all the available rapidity Y. Let us denote $T(r_1,r_0,Y)$ to be the scattering amplitude of the dipole (projectile) off a particular partonic realization $|\chi\rangle$ of another dipole (target). In this case, the $T(r_1,r_0,Y)$ is a random variable, whose probability distribution is related to the stochastic ensemble of dipole configurations endowed with a probability distribution which evolves with Y according to a master equation [12]. Therefore, the high energy parton evolution process can be viewed as a statistical process which is inspired by the reaction-diffusion process in statistical physics. The physical dipole-dipole scattering amplitude $\bar T(r_1,r_0,Y)$ is given by averaging over all possible dipole realizations of the target at rapidity Y [10],

$$\bar T=\langle T((\rho-\rho_s(Y))\rangle =\int {\rm d}\rho_s\; T(\rho-\rho_s(Y))\;P(\rho_s(Y)-\langle\rho_s(Y)\rangle) \tag{18}$$

where $\rho_s(Y)$ obeys Gaussian distribution [38, 39]:

$$P(\rho_s)\simeq\frac{1}{\sqrt{\pi\sigma^2}}\exp\left[-\frac{(\rho_s-\langle\rho_s\rangle)^2}{\sigma^2}\right] \tag{19}$$

with $\rho=\ln(r_0^2Q^2)$ and $\rho_s=\ln(r_0^2Q_s^2)$.

The gluon number fluctuations in the dilute regime result in fluctuations of the saturation scale from event to event, with the variance σ of the saturation scale

$$\sigma^2=\langle\rho_s^2\rangle-\langle\rho_s\rangle^2=DY \tag{20}$$

from numerical simulations of statistical models. $\rho_s=\ln(r_0^2Q_s^2(Y))$ is the position of the front. D is the diffusion coefficient, whose value is known only for $\alpha\to0$ [12]. To calculate the physical amplitude, we average the event-by-event scattering amplitude over all possible gluon number realizations [12, 22], which leads to a replacement of the geometric scaling resulting from the BK equation by a new scaling, the diffusive scaling, namely, $\langle T(r,Y)\rangle$ is a function of a single variable [40]

$$\langle T(r,Y)\rangle=f\left(\frac{\ln(r^2Q_s^2(Y))}{\sqrt{DY}}\right) \tag{21}$$

Now look at a dipole scattering off a highly evolved hadron in the diffusive scaling and geometric scaling region. In order to interpret the relevant physics in these two regions, let us look at the phase diagram of the hadron in the high energy limit shown in Fig. 3, where the longitudinal coordinate, $Y=\ln(1/x)$, is the rapidity of the hadron, transverse coordinate, ρ, is the logarithm of the transverse momentum of the gluons inside the hadron, and $\langle\rho_s\rangle$ is the averaged saturation line. The area at the left of the saturation line, $\rho<\langle\rho_s\rangle$, is the saturation region with high density large size gluons, of order $1/\alpha_s$, or $T\sim1$, where the non-linear effect becomes

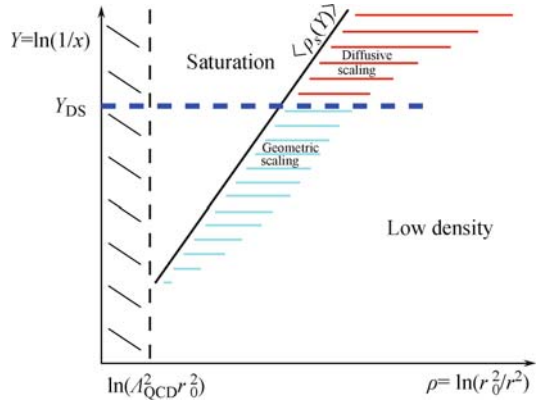

Fig. 3 The phase diagram of highly evolved hadron system [42].

important. At regime $\rho \gg \langle\rho_s\rangle$, the gluon density is low, where neither saturation nor fluctuation effects are important. The scattering amplitude shows color transparency in this region. There are two different regions within the transition region (see shadowing region in Fig. 3) which are separated by the rapidity scale $Y_{\rm DS}$, the geometric scaling regime and diffusive scaling regime, respectively. The dynamics of the QCD evolution are different in these two regions. At $Y \ll Y_{\rm DS}$, the dispersion is small $\sigma^2 \ll 1$, the effects of fluctuations can be neglected, and the evolution of the hadron is described to a good approximation by the BK equation. While at $Y \gg Y_{\rm DS}$, where $\sigma^2 \gg 1$, the fluctuations become important and the geometric scaling is replaced by the diffusive scaling [22, 41].

4 Possible diffusive scaling in deep inelastic scattering

We will now test the prediction Eq. (21). In order to study the diffusive scaling, we take the parameters, like diffusive coefficient D, saturation exponent λ, x_0, from Ref. [22]. In Ref. [22], the authors fitted the HERA experimental data by using the gluon number fluctuations effect on top of the Iancu, Itakula, Munier (IIM) model [43]. They found a sizeable value of diffusion coefficient, $D = 0.325$. This value is very close to the values found for D in the numerical solution of the pomeron loop equations [44] and in the (1+1) dimensional toy model [45]. The sizable value of D might indicate possible gluon number fluctuation existence in HERA data, which implies possible diffusive scaling in the available experimental DIS data, such as ZEUS, H1, E665 and NMC data.

The diffusive scaling behavior in Eq. (21) indicates a similar diffusive scaling for the deep inelastic scattering total cross-section

$$\sigma_{\rm tot}(x, Q^2) = \sigma_{\rm tot}(\tau) \tag{22}$$

with

$$\tau = \frac{\rho - \langle\rho_s\rangle}{\sqrt{DY}} \tag{23}$$

By fitting the HERA data, one can get

$$Q_s^2(x) = Q_0^2 \left(\frac{x}{x_0}\right)^{\lambda} \tag{24}$$

with reference scale $Q_0 = 1$ GeV, and the parameters $x_0 = 9.5 \times 10^{-7}$ and $\lambda = 0.198$. We would like to note that these group of data come from fitting the experimental data by only taking into account the light quarks (u,d,s) contribution. The left panel of Fig. 4 shows that the total cross-section $\sigma_{\rm tot}$ is a function of τ. The data are taken from different experiments with $x < 0.01$, ZEUS [30, 31], H1 [28], E665 [32] and NMC [33] collaborations. The data lie on the same curve, which indicates the possible diffusive scaling in the present available deep inelastic scattering data.

To study the heavy quarks contribution to the DIS total cross-section, the authors of Ref. [22] took the charm and bottom quarks into account, when they fitted the HERA data with the gluon number fluctuations effect on top of the IIM model. After including the heavy quarks contribution, they got $x_0 = 1.7 \times 10^{-7}$, $\lambda = 0.162$ and $D = 0.1105$. Now, we use this group of parameters to study the diffusive scaling in the deep inelastic scattering. The result is shown in the right panel of Fig. 4. Again, the data lie on a single curve, implying the possible diffusive scaling existence in the present available deep inelastic scattering data.

Note that with present available DIS experimental data we can not conclude the diffusive scaling in DIS, since the collision energy is not high enough and the geometric scaling is still important as present data. We believe that as collision energies increase the gluon number fluctuations would become clearer, which would lead to clearer diffusive scaling behavior. The LHC will provide a good opportunity to test whether the diffusive scaling

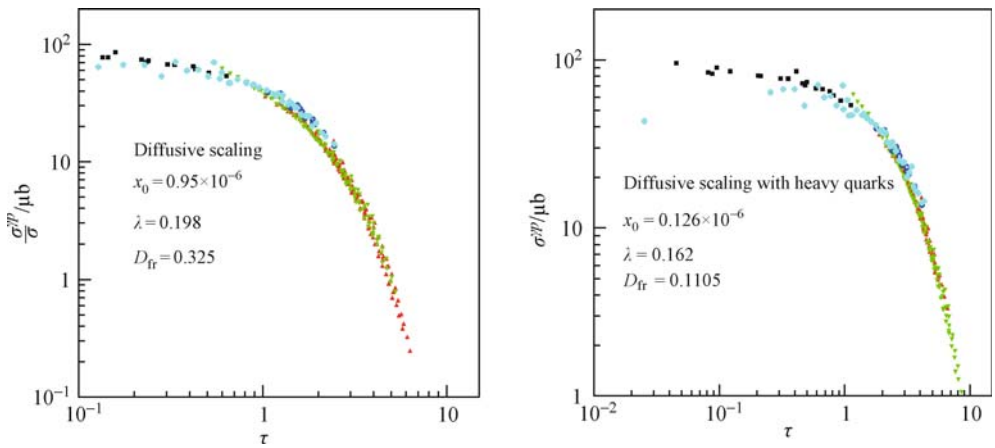

Fig. 4 The total cross-section is a function of a single variable, τ. The left panel denotes the total cross-section with only light quarks contribution. The right panel expresses the total cross-section with both light and heavy quarks contribution.

is suitable for the description of the experimental data at LHC energies.

References

1. I. Balitsky, Nucl. Phys. B, 1996, 463: 99
2. I. Balitsky, Phys. Lett. B, 2001, 518: 235
3. Yu. V. Kovchegov, Phys. Rev. D, 1999, 60: 034008
4. Yu. V. Kovchegov, Phys. Rev. D, 1999, 61: 074018
5. G. P. Salam, Nucl. Phys. B, 1995, 449: 5892
6. G. P. Salam, Nucl. Phys. B, 1996, 461: 512
7. A. H. Mueller and G. P. Salam, Nucl. Phys. B, 1996, 475: 293
8. E. Iancu and A. H. Mueller, Nucl. Phys. A, 2004, 730: 494
9. A. H. Mueller and A. Shoshi, Nucl. Phys. B, 2004, 692: 175
10. E. Iancu, A.H. Mueller, and S. Munier, Phys. Lett. B, 2005, 606: 342
11. W. C. Xiang, Phys. Rev. D, 2010, 81: 094004
12. E. Iancu and D. N. Triantafyllopoulos, Nucl. Phys. A, 2005, 756: 419
13. A. H. Mueller, A. I. Shoshi, and S. M. H. Wong, Nucl. Phys. B, 2005, 715: 440
14. E. Iancu and D. N. Triantafyllopoulos, Phys. Lett. B, 2005, 610: 253
15. W. C. Xiang, Eur. Phys. J. A, 2010, 46: 91
16. J. Jalilian-Marian, A. Kovner, A. Leonidov, and H. Weigert, Nucl. Phys. B, 1997, 504: 415
17. J. Jalilian-Marian, A. Kovner, A. Leonidov, and H. Weigert, Phys. Rev. D, 1999, 59: 014014
18. J. Jalilian-Marian, A. Kovner, and H. Weigert, Phys. Rev. D, 1999, 59: 014015
19. E. Iancu, A. Leonidov, and L. D. McLerran, Phys. Lett. B, 2001, 510: 133
20. E. Iancu, A. Leonidov, and L. D. McLerran, Nucl. Phys. A, 2001, 692: 583
21. E. Ferreiro, E. Iancu, A. Leonidov, and L. D. McLerran, Nucl. Phys. A, 2002, 703: 489
22. M. Kozlov, A. Shoshi, and W. C. Xiang, JHEP, 2007, 10: 020
23. K. Golec-Biernat and M. Wusthoff, Phys. Rev. D, 1999, 60: 114023
24. W. C. Xiang, D. C. Zhou, R. Z. Wan, and X. B. Yuan, Chin. Phys. C, 2009, 33: 98
25. E. Levin and K. Tuchin, Nucl. Phys. B, 2000, 573: 83
26. A. H. Mueller, arXiv: hep-ph/0111244, 2001
27. W. C. Xiang, Phys. Rev. D, 2009, 79: 014012
28. C. Adloff, *et al.* [H1 Collaboration], Eur. Phys. J. C, 2001, 21: 33
29. K. Golec-Biernat and M. Wusthoff, Phys. Rev. D, 1998, 59: 014017
30. J. Breitweg, *et al.* [ZEUS Collaboration], Phys. Lett. B, 2000, 487: 53
31. S. Chekanov, *et al.* [ZEUS Collaboration], Eur. Phys. J. C, 2001, 21: 443
32. M. R. Adams, *et al.* [E665 Collaboration], Phys. Rev. D, 1996, 54: 3006
33. M. Arneodo, *et al.* [E665 Collaboration], Nucl. Phys. B, 1997, 483: 3
34. E. A. Kuraev, L. N. Lipatov, and V. S. Fadin, Sov. Phys. JETP, 1977, 45: 199
35. Ya. Ya. Balitsky and L. N. Lipatov, Sov. J. Nucl. Phys, 1978, 28: 822
36. E. Iancu, C. Marquet, and G. Soyez, Nucl. Phys. A, 2006, 780: 52
37. K. Rummukainen and H. Weigert, Nucl. Phys. A, 2004, 739: 183
38. C. Marquet, G. Soyez, and B. W. Xiao, Phys. Lett. B, 2006, 639: 635
39. W. C. Xiang, Nucl. Phys. A, 2009, 820: 303C
40. Y. Hatta, E. Iancu, C. Marquet, G. Soyez, and D.N. Triantafyllopoulos, Nucl. Phys. A, 2006, 773: 95
41. W. C. Xiang, S. Q. Wang, and D. C. Zhou, Chin. Phys. Lett., 2010, 27: 072502
42. A. Shoshi, arXiv: 0708.4316, 2007
43. E. Iancu, K. Itakura, and S. Munier, Phys. Lett. B, 2004, 590: 199
44. G. Soyez, Phys. Rev. D, 2005, 72: 016007
45. E. Iancu, J. T. de Santana Amaral, G. Soyez, and D. N. Triantafyllopoulos, Nucl. Phys. A, 2007, 786: 131